Available online at www.sciencedirect.com
SCIENCE DIRECT
Trans. Nonferrous Met. Soc. China 18(2008) 28−32
Transactions of Nonferrous Metals Society of China
www.csu.edu.cn/ysxb/

Effect of Yb additions on microstructures and properties of 7A60 aluminum alloy

FANG Hua-chan(方华婵), CHEN Kang-hua(陈康华), ZHANG Zhuo(张 茁), ZHU Chang-jun(祝昌军)

State Key Laboratory of Powder Metallurgy, Central South University, Changsha 410083, China

Received 9 January 2007; accepted 28 April 2007

Abstract: Al-Zn-Mg-Cu-Zr alloys containing Yb were prepared by cast metallurgy. Effect of 0.30% Yb additions on the microstructure and properties of 7A60 aluminum alloys with T6 and T77 aging treatments was investigated by TEM, optical microscopy, hardness and electric conductivity measurement, tensile test and stress corrosion cracking test. The results show that the Yb additions to high strength Al-Zn-Mg-Cu-Zr aluminum alloys can produce fine coherent dispersoids. Those dispersoids can strongly pin dislocation and subgrain boundaries, which can significantly retard the recrystallization by inhibiting the nucleation of recrystallization and the growth of subgrains and keeping low-angle subgrain boundaries. Yb additions can obviously enhance the resistance to stress corrosion cracking and the fracture toughness property, and mildly increase the strength and ductility with T6 and T77 treatments.

Key words: Al-Zn-Mg-Cu alloys; ytterbium; mechanical properties; stress corrosion cracking; ageing

1 Introduction

Ultra-high strength Al-Zn-Mg-Cu aluminum alloys with low density and good machining properties have been widely used in the military and aerospace industries. However, this series of alloys are susceptible to stress corrosion cracking(SCC), which limits their usefulness [1−3]. People have done abundant researches in order to improve the combined properties of ultra-high strength Al-Zn-Mg-Cu aluminum alloys.

The Alcoa' T77 temper[4−5] can combine strength with resistance to corrosion favorably by precipitates in matrix presenting as T6 temper and precipitates at grain boundaries presenting as over-aged state by retrogression. However, intergranular cracking is still very notable, since a lot of precipitates concentrate at the grain boundaries after temper in the high-level alloyed ultra-high strength aluminum alloys.

In recent years, TANAKA et al[6−7] have remarkably improved the SCC resistance of the T6-tempered 7475 aluminum alloy and formed deformation reversion texture with low-angle grain boundaries by warm deformation processing. However, it is difficult to obtain the uniform warm deformation of ultra-high strength Al-Zn-Mg-Cu aluminum alloys, and the higher temperature deformation results in partial recrystallization.

Sc is the most effective micro-alloying element in aluminum alloys[8−9]. The effect can be more remarkable by replacing partial Sc with Zr to produce Al_3(Sc, Zr) dispersoids[10−11]. But expensive Sc additions are difficult to be extensively applied. The cheaper rare-earth element additions are being studied to replace Sc[12−13].

In this work, the authors found that the addition of rare-earth element Yb, less expensive than Sc, could obviously suppress the recrystallization, improve the strength and fracture toughness, as well as remarkably enhance SCC resistance of 7A60 alloy, and had applied two patents[14−15]. The effect of rare-earth element Yb on the microstructures, mechanical properties and SCC of ultra-high strength aluminum alloys are reported in the present work.

2 Experimental

The 7A60 alloys of chemical composition given in

Foundation item: Project(50471057) supported by the National Natural Science Foundation of China; Project(2005CB623704) supported by the National Basic Research Program of China; Project(NCET-04-0753) supported by the New Century Talented Professionals Program of Education Ministry, China; Project supported by the Key Lab of National Defense, China

Corresponding author: FANG Hua-chan; Tel: +86-731-8830714; E-mail: fanghc_1028@yahoo.com.cn

Table 1 were investigated. High purity aluminum (99.9%), magnesium (99.9%), zinc (99%), and Al-Zr, Al-Cu and Al-Yb alloys as raw materials were smelted into the alloys. The smelting temperature was kept at 700−740 ℃ and cast into *d*45 mm ingot in graphite mould.

The cast ingots were homogeneously annealed at 465 ℃ for 24 h, then were extruded at 410−430 ℃ into plate at 12.2 extrusion ratio. The extruded samples were held at 450 ℃ and 470 ℃ respectively for 1 h, then kept at 480 ℃ for 2 h for further solution treatment, then were quenched by cold water. The samples were tempered artificially with T6 and T77 treatment, respectively. Ageing process of all samples is listed in Table 2.

Table 1 Chemical composition of aluminum alloys (mass fraction, %)

Sample	Zn	Mg	Cu	Zr	Yb	Trace elements	Al
7A60	8.32	2.47	2.13	0.15	−	≤0.20	Bal
7A60+Yb	8.30	2.46	2.14	0.15	0.30	≤0.20	Bal

Table 2 Technical parameters of 7A60 and 7A60+Yb alloys

Sample	Aging
7A60-1 7A60+Yb-1	T6, 130 ℃, 24 h
7A60-2 7A60+Yb-2	T77, 130 ℃, 24 h+173 ℃, 3 h+130 ℃, 24 h

The hardness(HRB), tensile properties and electric resistance of the tempered plates were tested in HBRVU-187.5 sclerometer, CSS-44100 testing machine and SX1931 digital ohmmeter (four-probes method), respectively.

The samples for optical microscope observation were divided into two groups. The first was anode coating after being electro-polished and then the recrystallization behavior of the alloy was observed by optical polarized microscopy(OM) on a Polyver-Met optical microscope. The second was etched with modified Keller's reagent and then the growth of subgrains was observed by OM. Thin foils for TEM were prepared by twin jet-polishing in electrolyte solution of HNO_3 and methyl alcohol (volume ratio, 1:3) and then were examined on H-800 transmission electron microscope.

Stress corrosion crack growth rate measurements were carried out in double cantilever beam(DCB) specimens in 3.5% NaCl solution at (35±1) ℃ according to the Chinese GB/T12445.1—1990 specification. For stress intensity factor K_I corresponding to crack expansion in stress corrosion, the dimension of samples accorded with $B \geqslant 2.5(K_{IC}/\sigma_{0.2})^2$ and $(1-a) \geqslant 2.5(K_{IC}/\sigma_{0.2})^2$.

3 Results

3.1 Tensile properties, hardness, electric resistance and fracture toughness

The tensile properties, hardness and electronic resistance of the T6 and T77-tempered alloys are shown in Table 3. Yb additions can moderately improve the hardness, strength, elongation, fracture toughness and decrease the electronic resistance of ultra-high strength 7A60 alloy in T6 and T77 temper. According to the relationship between electric resistance and resistance to stress corrosion, SCC resistance of 7A60 alloy could be improved to some degree with Yb additions.

3.2 Stress corrosion susceptibility

The effects of Yb additions on the stress corrosion cracking growth rate of DCB samples of T6 and T77-tempered 7A60 alloy are shown in Fig.1. It is found that the resistance to SCC of 7A60 alloy with Yb additions is obviously improved.

In peaking ageing state (Fig.1(a)), the growth rate of SCC of 7A60 alloy is high. Yb additions can remarkably decrease the growth rate of SCC of the alloy and enhance the critical stress intensity K_{ISCC} from 9.8 MPa·m$^{1/2}$ to 17.0 MPa·m$^{1/2}$.

In retrogression and re-ageing state (Fig.1(b)), the SCC resistance of 7A60+Yb-2 alloys is obviously enhanced compared with that of 7A60-2 alloys. Moreover, the growth rate of SCC of 7A60-2 alloy with T77-temper is higher than that of 7A60+Yb-1 alloy with T6-temper, and the critical stress intensity K_{ISCC} of 7A60+Yb-1 alloy with T6-temper is 17.0 MPa·m$^{1/2}$, which is higher than that of 7A60-2 alloy with T77-temper.

Table 3 Mechanical properties of 7A60 and 7A60+Yb alloys

Sample	Aging	σ_b/MPa	$\sigma_{0.2}$/MPa	δ_{10}/%	HRB	ρ/(Ω·nm)	K_{IC}/(MPa·m$^{1/2}$)
7A60-1	T6	711.7	685.4	8.9	96.7	59.6	23.7
7A60+Yb-1	T6	728.7	698.2	10.1	99.1	55.6	32.4
7A60-2	T77	696.2	680.9	9.3	96.0	46.3	22.1
7A60+Yb-2	T77	702.8	698.5	9.6	98.5	44.6	31.2

3.3 Microstructures

Fig.2 shows the effects of Yb additions on the optical microstructure of 7A60 alloy. During the high temperature solution treatment, 7A60 alloy containing Zr partially recrystallizes (Figs.2(a) and (c)) and 7A60+Yb alloy maintains the fiber-like nonrecrystallization morphology (Figs.2(b) and (d)). That is, the recrystallization of Al-Zn-Mg-Cu alloy can not be completely inhibited only by Zr additions. However, Yb and Zr additions can remarkably enhance the resistance to recry-

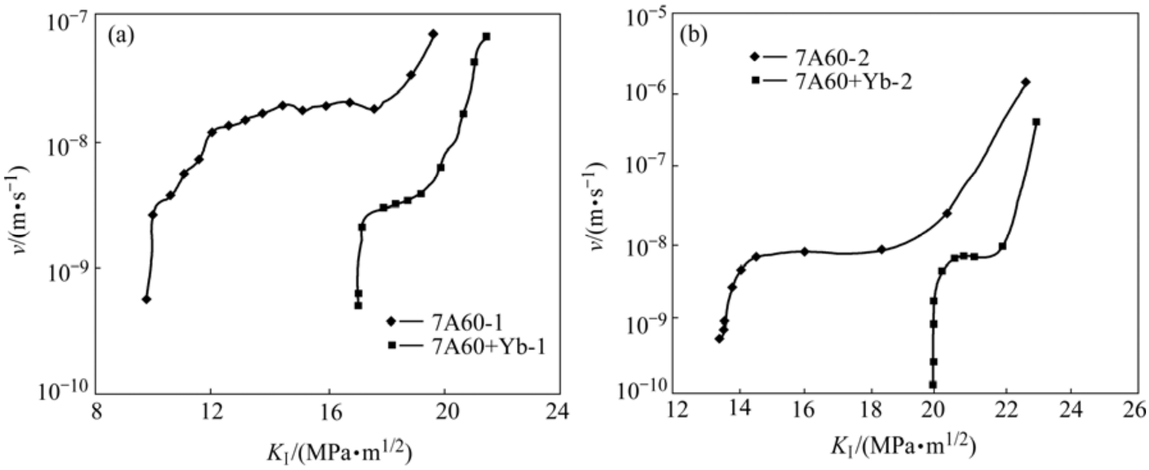

Fig.1 Relationships between SCC growth rate and stress intensity factor in dropwise 3.5% NaCl environment for 7A60 alloys with Yb addition in different ageing treatments: (a) T6; (b) T77

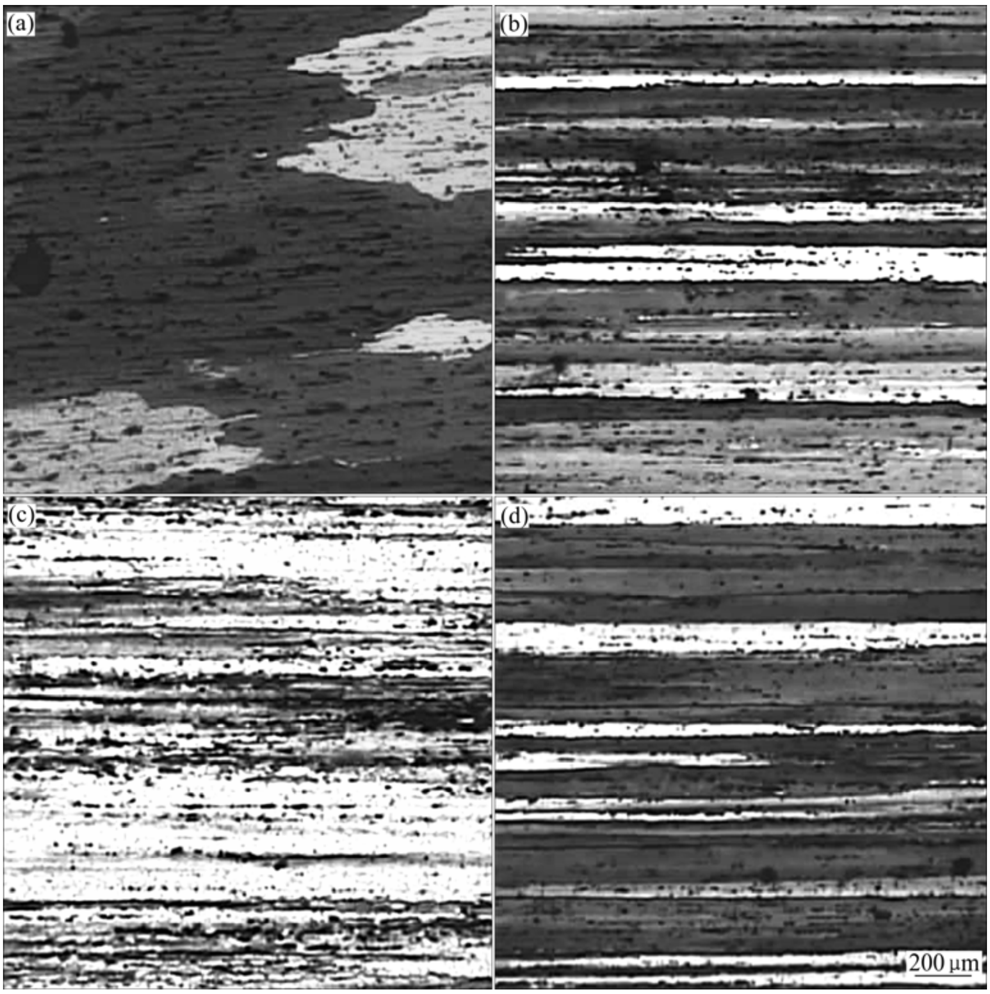

Fig.2 Optical microstructures of two studied alloys with solution treatment: (a) 7A60-1(L-T surface); (b) 7A60+Yb-1(L-T surface); (c) 7A60-1(L-S surface); (d) 7AYb+Yb-1(L-S surface)

stallization of Al-Zn-Mg-Cu alloy.

Fig.3 shows the effects of Yb additions on the optical microstructure of 7A60 alloy after being etched with modified Keller's reagent. The subgrains of 7A60 alloy containing Zr grow up (Fig.3(a)). Structure with adding 0.30%Yb of 7A60 alloys presents complete fiber characteristics, and no subgrain growth occurs (Fig.3(b)). It is found that the growth of subgrains of 7A60 alloy with Yb additions is obviously restrained.

TEM images of T6-tempered 7A60+Yb alloy are shown in Fig.4. It can be seen from Figs.4(a)−(c) that Al_3Zr bar particles and 10−50 nm spherical dispersoids coherent with the matrix disperse in the grain and at the grain boundary. The spherical coherent dispersoids

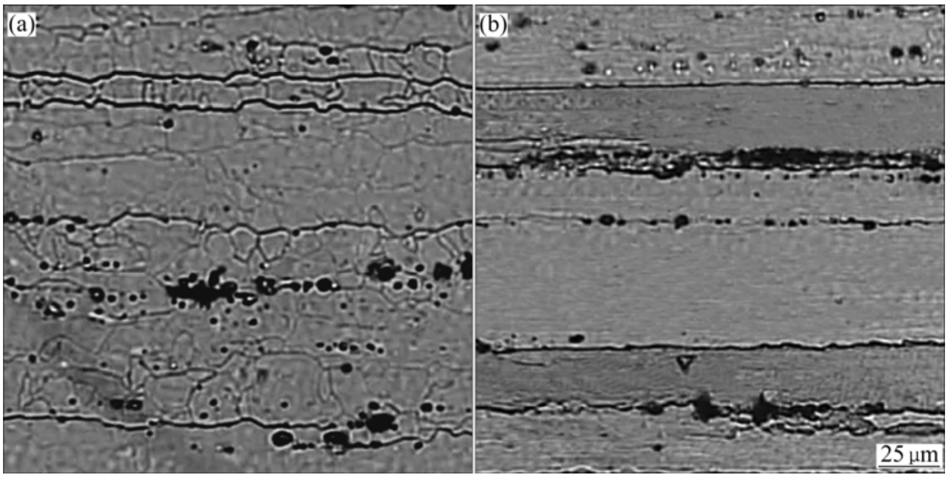

Fig.3 Optical microstructures of two studied alloys with T6 ageing treatment: (a) 7A60-1; (b) 7A60+Yb-1

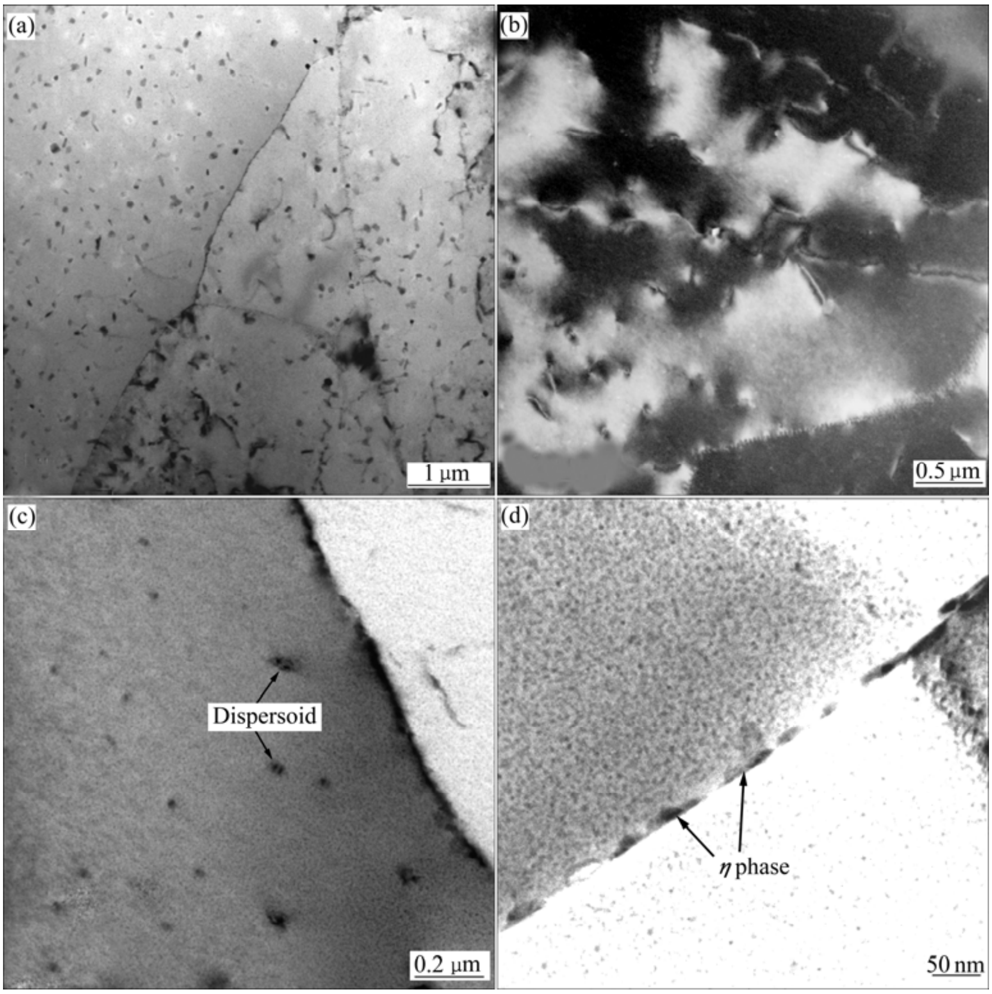

Fig.4 TEM images of T6-tempered Al-Zn-Mg-Cu-Zr alloy (7A60+Yb)

contain Yb, Zr and Al according to EDX analysis. The dislocation and subgrain boundaries can be pinned by the fine coherent spherical dispersoids and therefore the subgrains are stabilized, as shown in Figs.4(a) and (b), thus inhibiting subgrains growth and recrystallization. As shown in Fig.4(d), the coarse and discontinuous 50−80 nm equilibrium precipitates exist at the grain boundaries in the T6-tempered alloy, and around the grain boundaries exists the narrow precipitate-free zone with width of 10 nm, which can reflect the characteristics of low angle grain boundary in unrecrystallized micro-structure.

4 Discussion

As mentioned above, Yb additions to 7A60 alloy can moderately improve the strength, ductility, fracture toughness, as well as remarkably enhance the SCC resistance of 7A60 alloy with T6 and T77 treatments. The effects of Yb additions result from a lot of tiny coherent dispersions containing Yb, Zr and Al in the alloy. The fine coherent dispersoids have precipitation strengthening effect. The dispersoids can retard recrystallization and subgrains growth, as shown in Figs.4(a), (b) and (c), and result in substructure strengthening. Both effects contribute to the improvement of the strength.

The coherent dispersions in 7A60+Yb alloy can also stabilize the deformation reversion microstructure (Figs.2(b) and (d)) with low-angle subgrain boundaries (Fig.3(b)) or grain boundaries by inhibiting the movement of the subgrain boundaries and retarding the transformation of subgrain boundaries to high-angle grain boundaries. Since the low-angle grain boundary energy is much smaller than the high-angle one, the energy difference between grain boundaries and grain interior can be reduced in the unrecrystallized 7A60+Yb alloy. So, the aggregation of the precipitates at the grain boundary can be decreased due to the energy decrease in the unrecrystallized 7A60+Yb alloy. Moreover, coarse and discontinuous grain boundaries $\eta(MgZn_2)$ precipitates (Fig.4(c)) retard anodic dissolution and decrease the stress corrosion cracking susceptibility. In addition, the coherent dispersoids can not be sheared and can be only bypassed by the dislocation, so preventing the coplanar dislocation slip and improving the deformation uniformity in grains. Both effects of coherent dispersoids are beneficial to the resistance to grain boundary cracking, and result in the improvement of the ductility and SCC resistance.

5 Conclusions

1) Yb additions can moderately improve the strength, ductility, fracture toughness, as well as remarkably enhance the SCC resistance of 7A60 alloy with T6 and T77 treatment.

2) Yb additions to 7A60 alloy can produce fine coherent dispersoids that can effectively inhibit the movement of dislocation and subgrain boundaries, retard the recrystallization and keep low-angle subgrain boundaries.

References

[1] JAME T S, JOHN L, WARREN H H Jr. Aluminum alloys for aerostructures [J]. Advanced Materials and Process, 1992, 10: 17−20.

[2] DAVID A L, RAY M H. Strong aluminum alloy shaves airframe weight [J]. Advanced Materials and Process, 1991, 10: 46−49.

[3] LIU J, KULAK M. A new paradigm in the design of aluminum alloys for aerospace applications [J]. Materials Science Forum, 2000, 331/337: 127−140.

[4] BROWN M H. Three steep aging to obtain high strength and corrosion resistance in Al-Zn-Mg-Cu alloys [P]. US 4477292, 1984−10−16.

[5] FENG Chun, LIU Zhi-yi, NING Ai-lin, LIU Yan-bin, ZENG Su-ming. Retrogression and re-aging treatment of Al-9.99%Zn-1.72%Cu-2.5%Mg-0.13%Zr aluminum alloy [J]. Trans Nonferrous Met Soc China, 2006, 16(5): 1163−1170.

[6] TANAKA H, ESAKI H, YAMADA K, SHIBUE K, YOSHIDA H. Improvement of mechanical properties of 7475 based aluminum alloy sheets by controlled warm rolling [J]. Sumitomo Light Metal Reports, 2004, 45(1): 41−48.

[7] TANAKA H, ESAKI H, YAMADA K, SHIBUE K, YOSHIDA H. Mechanical properties of 7475 based aluminum alloy sheets with fine subgrain structure [J]. Journal of Japan Institute of Light Metals, 2002, 52(11): 553−558.

[8] RØYSET J, RYUM N. Scandium in aluminum alloys [J]. International Materials Review, 2005, 50(1): 19−44.

[9] WU Y L, FROES F H, LI C G, ALVEAREZ A. Microalloying of Sc, Ni, and Ce in advanced Al-Zn-Mg-Cu alloy [J]. Metallurgical and Materials Transactions, 1999, 30A: 1017−1024.

[10] DAI Xiao-yuan, XIA Chang-qing, LIU Chang-bin. Effect of trace Sc on microstructures and properties of Al-Zn-Mg-Cu-Zr based alloys [J]. Mining and Metallurgical Engineering, 2004, 24(3): 59−61, 63. (in Chinese)

[11] HE Yong-dong, ZHANG Xin-ming, YOU Jiang-hai. Effect of minor Sc and Zr on microstructure and mechanical properties of Al-Zn-Mg-Cu alloy [J]. Trans Nonferrous Met Soc China, 2006, 16(5): 1228−1235.

[12] YANG Jun-jun, NIE Zuo-ren, JIN Tou-nan, RUAN Hai-qiong, ZUO Tie-yong. Form and refinement mechanism of element Er in Al-Zn-Mg alloy [J]. The Chinese Journal of Nonferrous Metals, 2004, 14(4): 620−626. (in Chinese)

[13] KARNESKY R A, DALEN ME, DUNAND D C, SEIDMAN D N. Effects of substituting rare-earth elements for scandium in a precipitation-strengthened Al-0.08 at.%Sc alloy [J]. Scripta Materialia, 2006, 55(5): 437−440.

[14] CHEN Kang-hua, HUANG Lan-ping, FANG Hua-chan, ZHANG Zhuo. Anti-recrystallized Al-Zn-Mg-(Cu) alloys [P]. CN 200610031119.0, 2006−01−09.

[15] CHEN Kang-hua, FANG Hua-chan, ZHANG Zhuo, ZHU Chang-jun, HUANG Lan-ping. High strength, high toughness and high corrosion resistant Al-Zn-Mg-(Cu) alloys [P]. CN 200610136903.9, 2006−12−19.

(Edited by LI Xiang-qun)